Scientia Iranica A (2015) 22(4), 1411–1421

Sharif University of Technology
Scientia Iranica
Transactions A: Civil Engineering
www.scientiairanica.com

Evaluation of the main factors influencing the behavior of strip footings on geogrid reinforced soils

S.M. Mir Mohammad Hosseini and M.M. Salehi*

Amirkabir University of Technology, Tehran, Department of Civil and Environmental Engineering, Iran.

Received 3 December 2013; received in revised form 22 September 2014; accepted 27 September 2014

KEYWORDS
Bearing capacity;
Geogrid;
Numerical analysis;
Strip footing;
Reinforced soil.

Abstract. Soils reinforced by geogrids exhibit different behavior, compared to unreinforced soils, due to having high tensile strength elements. In this paper, the main factors influencing the behavior of such reinforced soil under a strip footing are investigated and discussed. A numerical model for the reinforced soil is developed using FLAC-2D finite difference software. The model is calibrated, and then different important factors, such as width, number, distance and depth of the first layer of geogrid, are studied and evaluated. The qualitative behavior of the reinforced soil under different conditions of reinforcement elements is also studied in this work. The results of several analyses show that the optimum depth of the first layer of geogrid is one fourth of the footing width, and the other layers would have effective role up to 1.75 times of the width. Also, the distance between geogrid layers needs to be decreased in case of increasing their number whose optimum value is less than half of the footing width. The geogrid width and its tensile strength have considerable effect on the behavior of the reinforced soil when geogrid layers are in optimum position.

1. Introduction

In some cases, facing with problematic soils or weak bearing capacity grounds on one hand, and the limitation of the footing dimensions on the other hand causes a great challenge for foundation engineers. Reinforcing soils with geogrids may be a suitable and economic way of increasing the bearing capacity and reducing settlements. Adding reinforcement elements with high tensile strength to soils that normally have no tensile strength, provides a composite material which has different behavior, compared to unreinforced soils.

Many experimental and numerical studies have been performed to investigate the behavior of reinforced soil foundation for various types of reinforcement (e.g. [1-6]). The first study reported in the literature was conducted by Binquet and Lee to evaluate the bearing capacity of sand reinforced using metal strips [7]. Since then, several studies were conducted to evaluate the influences of the geogrid elements on behavior of the granular soils under strip loading. Among them, Huang and Tatsauka [8], Khing et al. [9], Omar et al. [10], Shin and Das [11], Shin et al. [12], Patra et al. [13], Kumar et al. [14], Basudhar et al. [15], Sharma et al. [16] and Abu-Farsakh et al. [17] can be mentioned. The results of studies reported in the literature showed that the bearing capacity of the soil improves when reinforced by geogrids, and that better improvements are obtained when the reinforcement is placed within a certain depth. However, the optimum amounts of the effective parameters are not the same, depending on the physical and mechanical characteristics of the soil and the geogrid elements used in the studied models. According to the literature review, it can be concluded that: (i) The first reinforcement layer should be located close to the bottom of the footing at an optimum depth of $0.2B$-$0.5B$ (B is the width of footing); (ii) The optimum vertical spacing of the reinforcement layers

*. *Corresponding author. Tel.: +98 21 66400243*
E-mail addresses: mirh53@yahoo.com (S. Majdedin Mir Mohammad Hosseini); mm.salehi@aut.ac.ir (M.M. Salehi)

was found to be $0.2B$-$0.5B$; (iii) The maximum total depth of the reinforcement layers varied from $1.0B$ to $2.0B$. Thus, due to the scattered results of the research works and wide-spread usage of the geogrids in soil improvements, further investigations on the role of the effective parameters, in this method, are necessary. In addition, a qualitative study of the topic would be helpful in understanding the effects of various parameters.

In this paper, a numerical model has been introduced to investigate the influence of the main factors on the behavior of a strip footing rested on geogrid reinforced sand. The finite difference package of the FLAC is used to analyze the numerical model. Using this model, the developed stresses and strains at different zones of the soil can be detected and observed. Considering the displacement vectors of the soil particles under different geogrid layer positions, the mechanism of the soil improvement is studied and explained. In the present research, some practical information about the optimum position of a geogrid layer is investigated. Furthermore, effect of increasing the number of geogrid layers on bearing capacity of the soil is studied by changing depth of the first layer and the distance of the geogrid layers.

2. Geometric parameters

In Figure 1, a strip footing with dimensions $B \times L$ (width×length) under a surcharge of q, rested on a soil reinforced by n geogrid layers with dimensions l (length) and b (width), is shown. The geogrid spacing is h, and the depth of the first layer is u, measured from the top of the soil layer. The depth of the last layer from the soil surface is denoted by d.

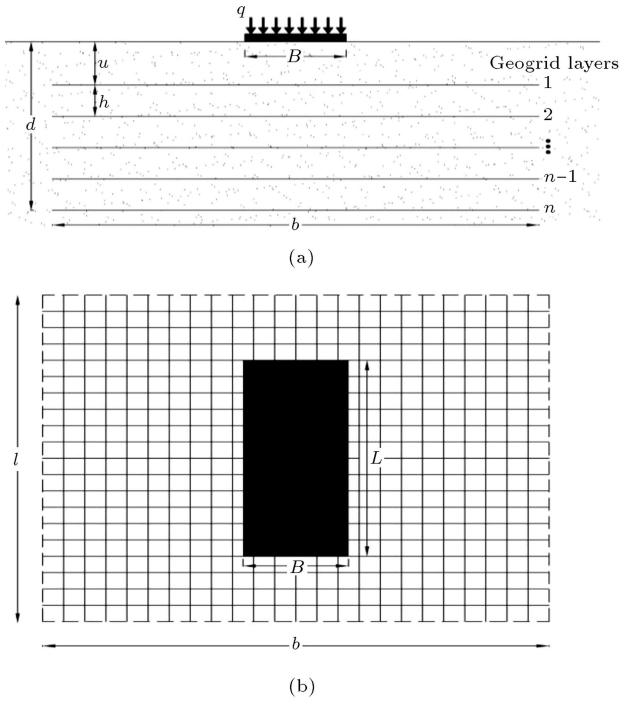

Figure 1. Geometric parameters of a strip footing on geogrid-reinforced soil: a) Section; and b) plan.

Generally, application of the load on the footing causes the stresses to increase inside the soil, and the settlement builds up gradually, leading to failure of the soil beneath the footing. In order to investigate the effect of the reinforcement on the bearing capacity of the soil, a dimensionless parameter has been defined as follows:

$$\mathrm{BCR}_u = \frac{q_{u(R)}}{q_u}, \tag{1}$$

where, $q_{u(R)}$ and q_u are the soil bearing capacities after and before reinforcement, respectively.

3. The numerical model and its validity

To investigate the behavior of unreinforced or geogrid-reinforced soil under different conditions, and to evaluate the behavioral parameters qualitatively and quantitatively, a numerical model is developed using the finite difference FLAC software. Since a strip footing is used and the plain strain condition is governed, a two dimensional model is developed. The numerical model accuracy has been analyzed and verified, using the physical model previously developed in the soil mechanics of Amirkabir University of Technology [18]. In order to use the experimental data, characteristics and dimensions have been used similar to the ones used in the physical model.

3.1. The soil media

The soil behavior has been modeled using hyperbolic model, coupled with Mohr-Coulomb failure envelop. In this non-linear model, the soil elasticity modulus is function of stress, which is altered by the loading conditions:

$$E = [1 - R_f S_l]^2 K P_a \left(\frac{\sigma_3}{P_a}\right)^n, \tag{2}$$

where P_a is the atmospheric pressure, and S_l is the stress level defined by the following equation:

$$S_l = \frac{\sigma_1 - \sigma_3}{(\sigma_1 - \sigma_3)_f}. \tag{3}$$

The differences between failure stresses, based on Mohr-Columb failure criteria are expressed as follows:

$$(\sigma_1 - \sigma_3)_f = \sigma_3 \left(\frac{1 + \sin\Phi}{1 - \sin\Phi} - 1\right) - 2c\sqrt{\frac{1 + \sin\Phi}{1 - \sin\Phi}}, \tag{4}$$

K (modulus number), n (exponent number) and R_f (failure ratio) are the model parameters. These pa-

Table 1. Physical characteristics of soil [18].

C_u	2.18	G_s	2.67
C_c	1.38	$(\gamma_d)_{\min}$	1.424 kN/m^3
D_{10}	0.75 mm	$(\gamma_d)_{\max}$	1.698 kN/m^3
D_{50}	1.54 mm	(γ_d)	1.61 kN/m^3

Table 2. Soil numerical model parameters.

K	n	R_f
757.28	0.4634	0.8927

Table 3. Results of triaxial tests [18].

σ_3 (kPa)	$(\sigma_1 - \sigma_3)_f$ (kPa)	Φ
25	115	43.7
50	215	42.8
75	316	42
100	397	41.5
150	579	40.6
200	739	40.1
250	876	39.3

rameters are calculated, using triaxial tests, for the granular soil with characteristics shown in Table 1. The values are shown in Table 2.

By increasing the confined pressure, the change in angle of internal friction of the soil (based on the triaxial test results shown in Table 3, and linear regression) is expressed as follows:

$$\Phi = 43.67 - 0.0184\sigma_3. \tag{5}$$

In dense granular materials, dilation plays significant role in the behavior of the soil. This key parameter is defined as dilation angle, ψ. In this study, the soil dilation angle, according to Yin et al. studies [19] and model verification results, is assumed to be half of the soil internal friction angle.

Taking into account the symmetrical condition of the model, half of the soil media (i.e. 80 cm width and 56 cm height) has been modeled (Figure 2). The boundary conditions have been defined as free displacement in Y direction and fixed condition in X direction. Besides, the base of the model has been fixed in both directions, X and Y.

The footing model has also been defined by fixing degrees of freedom of the nodes in both X and Y directions. Thus, the footing with 5 cm width is similar to a rigid and rough surface. The load is applied to the whole footing nodes using 2×10^{-6} m/step large displacement velocity vectors.

3.2. Geogrid

The cable element in FLAC package is able to model the tensile strength of the reinforcement elements and

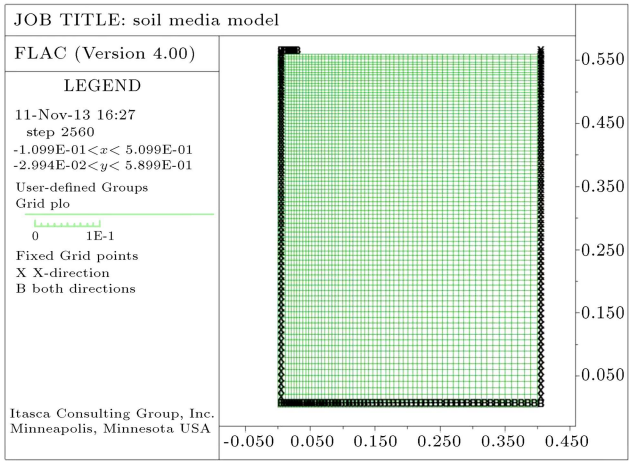

Figure 2. The numerical model of the soil media and its boundary conditions.

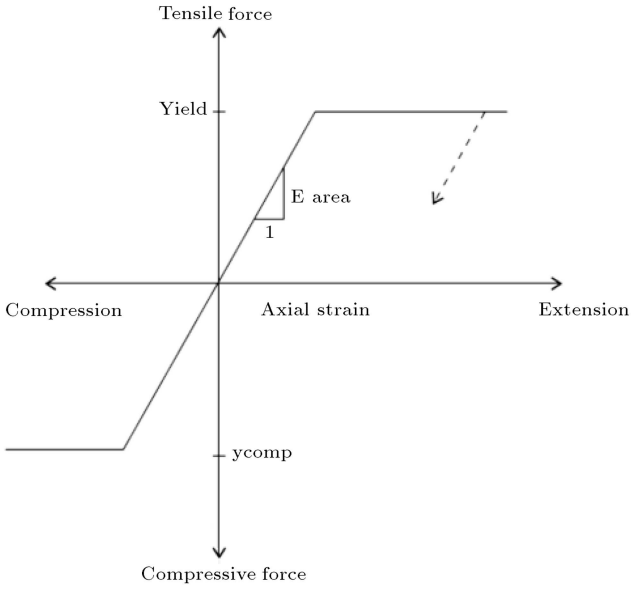

Figure 3. Axial behavior of a cable element in extension and compression.

their interaction with soil. Thus, cable element is used in this paper as geogrid reinforcement. The axial behavior of the cable element, similar to the rod element, can be expressed by the same parameters as cross-section, initial length, modulus of elasticity, and its ultimate tensile strength (Figure 3).

The shear behavior of the cable element in a continuum media and its interaction with the surrounding media have been defined by a spring model at two ends of the cable element. In other words, it has been defined as relative displacement between the cable element and the surrounding media.

$$\frac{F_S}{L} = K_{\text{bond}}(u_c - u_m). \tag{6}$$

In the above equation, F_s is the shear force developed along the grouting media, K_{bond} is the shear stiffness of

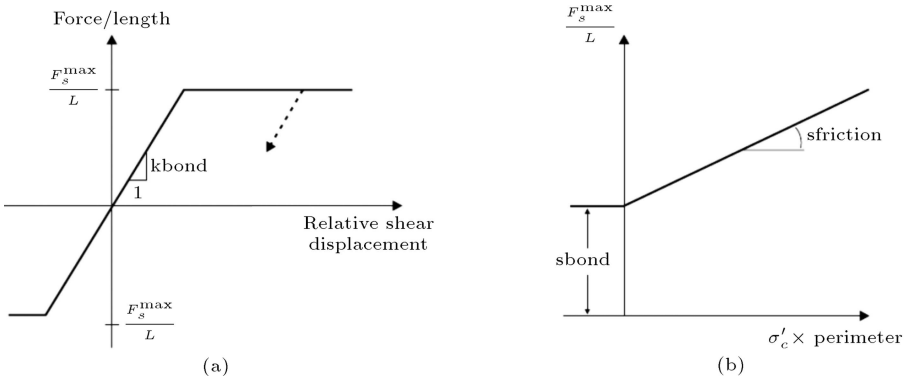

Figure 4. The shear behavior of a cable element and the surrounding media: a) The shear force of the grouting medial versus relative displacement; and b) the shear strength of the grouting media criterion.

the grouting media, L is the length of the cable element, and u_c and u_m are the axial displacements of cable and soil, respectively. The maximum shear force developed in the grouting media, per unit length of the element, can be defined as a function of cohesion and angle of internal friction of the grouting media.

$$\frac{F_S^{\max}}{L} = S_{\text{bond}} + \sigma'_c \times \tan(S_{\text{friction}}) \times \text{Perimeter}, \quad (7)$$

where S_{bond} is the cohesion or the inherent strength of the grouting media, σ'_c is the normal stress, S_{friction} is the angle of internal friction, and perimeter is the circumference of the element (Figure 4).

In order to build the model, the geogrid with properties shown in Table 4, and the soil-geogrid interaction theoretical equations with parameters shown in Table 5 have been used.

3.3. Validation of the model

The numerical model is verified using the similar experimental model which has already been developed in soil labs for both reinforced and unreinforced conditions. Figure 5 shows the variations of the developed stresses beneath footing versus the settlements for reinforced and unreinforced soils.

Table 4. Physical properties of the selected geogrid.

Weight (gr/m^2)	450
Mesh dimensions (mm)	6×6
Mesh thickness (mm)	2.05
Percent of open space (POA)	75
Tensile strength of the max. load (kN/m)	2.16

Table 5. Characteristics of the geogrid numerical model.

S_{bond} (N/m)	K_{bond} (N/m^2)	S_{friction}	Elastic modulus (N/m^2)	Tensile yield strength (N/m)
0	10^9	30	36363	2160

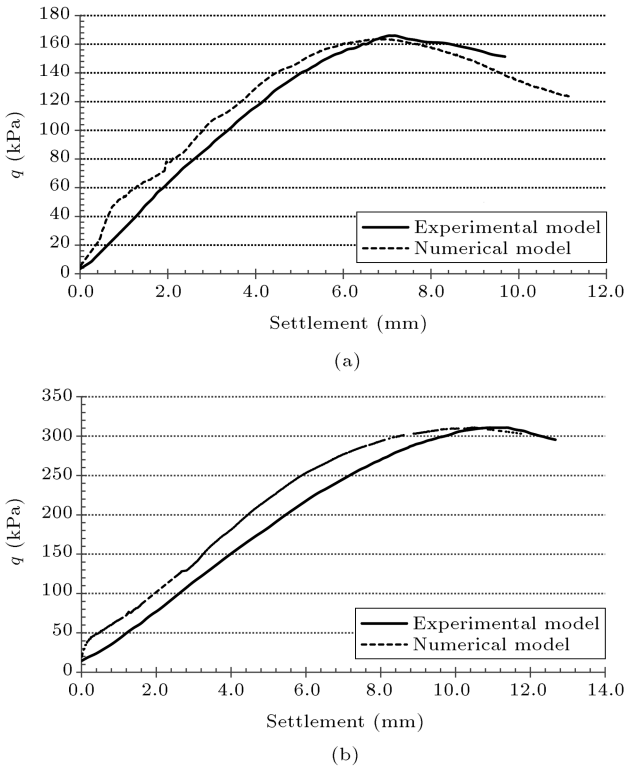

Figure 5. Comparison between results of the existing physical model and the present numerical model: a) Unreinforced soil; and b) one geogrid layer reinforced soil.

The bearing capacities obtained from experimental and numerical models are in relatively good agreement, which indicates the validity and reliability of the present model.

4. Parametric analyses results

4.1. Effect of the first layer depth

By changing the geogrid depth (u) from $0.125B$ to $2B$ (where B is the foundation width), the effect of the first geogrid layer depth on the bearing capacity has been evaluated by calculating BCR_u ratios (Figure 6). To make sure that the maximum confinement between

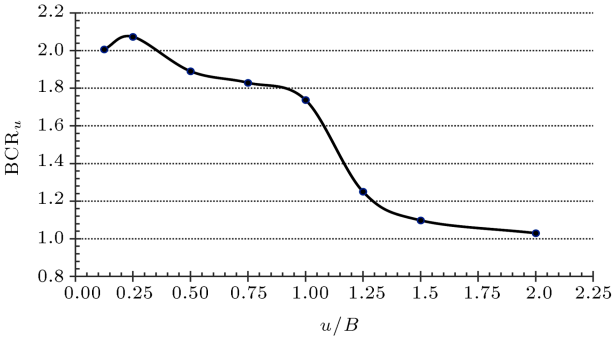

Figure 6. Variations of (BCR_u) versus the depth of the first geogrid layer (u/B) for $b/B = 15$ (where b is the geogrid width, and B is the foundation width).

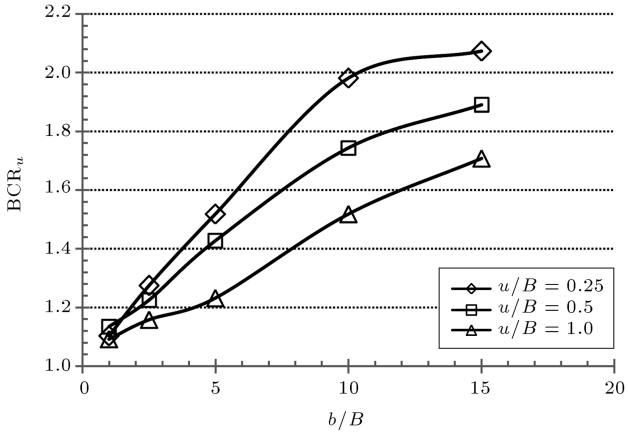

Figure 8. Variations of the ultimate bearing capacity ratio (BCR_u) against the ratio of the geogrid width to the foundation width (b/B).

soil and geogrid has been occurred, the geogrid width (b) has been considered equal to $15B$. As can be seen, initially a small increase in bearing capacity occurs by increasing u/B, followed by a decreasing trend. At the end, BCR_u tends to get a constant value. Smaller amounts of the bearing capacity, in u/B, less than $0.25B$ may be due to smaller overburdens under which the maximum shear strength of geogrid cannot be mobilized and, as result, the pull out condition may happen.

The increase in the slope of the above graph, after $u/B = 1$, shows the sudden change in the bearing capacity that could be attributed to the change in failure mechanism of reinforced soil. The failure wedge for u/B values less than 1 continues down to the reinforced element, but when the geogrid layer is placed at a deeper level, the failure wedge occurs above it, and the reinforced layer, in fact, acts as a rigid boundary (Figure 7).

4.2. Effect of the geogrid width

To investigate the effect of the geogrid layer width on the ultimate bearing capacity of the foundation, geogrids are placed at 3 different depths; $u/B = 0.25$, 0.5, and 1; and with changing the geogrid width from $1B$ to $15B$, the ratios of BCR_u are calculated for each case. The results show that the ultimate bearing capacity (BCR_u) will increase by increasing the geogrid width (Figure 8). The increase in bearing capacity could be due to the interaction between geogrid and soil in the form of pull out force (for $u/B \leq 1$) and the increase of geogrid fixing length.

Thus, if the geogrid has enough width to cover the whole failure wedge width and prevent the failure wedge from developing towards the soil surface, the bearing capacity would increase considerably. Figure 9 illustrates this fact by showing the displacement vectors of soil particles beneath the foundation.

Analyses results show that if the geogrid width is $10B$, for the placement depths of $0.25B$, $0.5B$, and $1B$, about 96, 92, and 90 percent, respectively, of the ultimate bearing capacity of reinforced soil by the geogrid width of $15B$ are attained. Also, using the geogrid width of $5B$, about 75 percent of the ultimate bearing capacity of the reinforced soil by the geogrid width of $15B$ can be achieved.

4.3. Effect of the number and distance of the geogrid layers

In some cases, due to soil conditions and the magnitude of applied load, more bearing capacity improvement is required. Thus more geogrid layers may be used. In such cases, the optimum number of geogrid layers, as well as the depth of the first layer, plays an important role. To study this factor, the number of geogrid layers is increased up to 11 for different spacing ratios ($h/B = 0.125$ up to 1.25). All analyses are

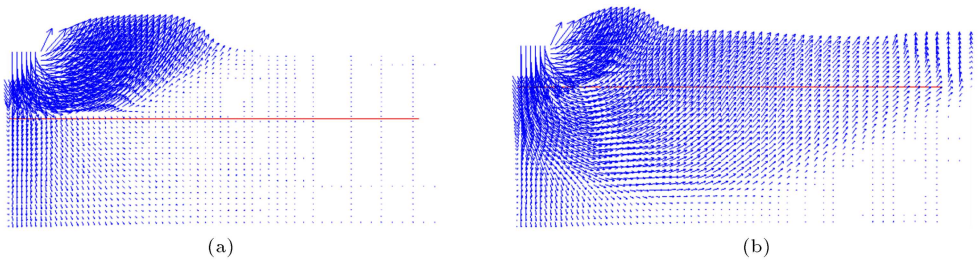

Figure 7. Displacement vectors of soil particles beneath foundation together with geogrid element at two depths: a) $u/B = 1.25$; and b) $u/B = 0.75$.

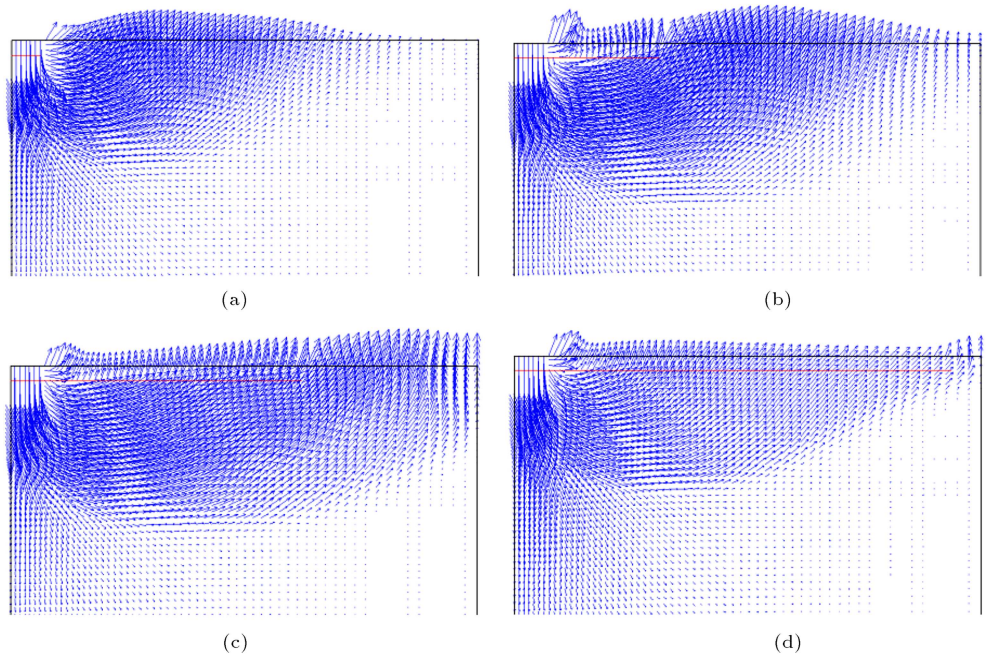

Figure 9. Displacement vectors of soil particles beneath foundation reinforced by a geogrid layer with $u/B = 0.25$: a) $b/B = 1$; b) $b/B = 5$; c) $b/B = 10$; and d) $b/B = 15$.

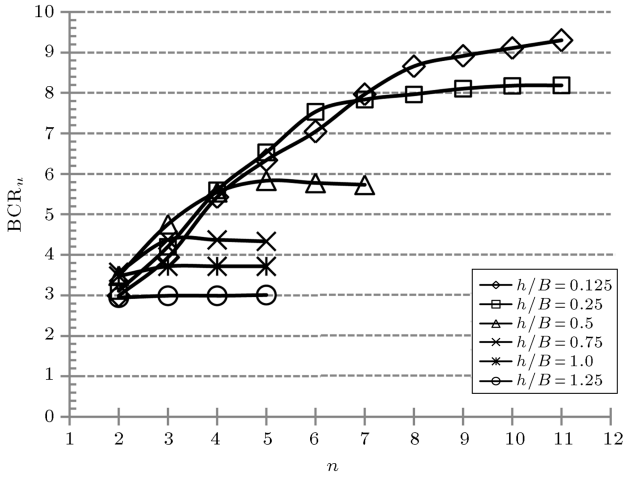

Figure 10. Variations of the ultimate bearing capacity ratio (BCR$_u$) versus number of the geogrid layers (n) for different spacing ratios (h/B) at $u/B = 0.25$.

done for $b/B = 15$ and three values of u/B (0.25, 0.5 and 1).

The effect of increasing geogrid layers for different distances is investigated first, while $u/B = 0.25$. As can be seen in Figure 10, the increasing number of geogrid layers with large spacing does not have a significant effect on the bearing capacity. In large spacing, the lower layers do not have any role in controlling the failure wedge (Figure 11). Nevertheless, the geogrid layers with small spacing may have no effect on the bearing capacity, if their number exceeds a certain value.

In Figure 12, the variations of BCR$_u$, due to increasing the number of geogrid layers of different spacing values have been shown. In this case, the depth of first layer geogrid is increased to $0.5B$. It can be seen that the general trend is the same as for $u/B = 0.25$, but the bearing capacity is reduced, which could be due to placing the first layer out of the optimum depth of $0.25B$. This reduction in large geogrid spacing ($h/B > 0.5$) is relatively constant and about 20-30%; for small geogrid spacing, it changes from 5%, for a few numbers of layers, up to 25%, for more number of layers.

Variation of the ultimate bearing capacity ratio (BCR$_u$) against the number of geogrid layers, while the depth of the first geogrid layer is equal to the foundation depth ($u/B = 1$), has been plotted in Figure 13. As can be seen, for this condition neither increasing the geogrid layers nor changing their distances has any effect on the bearing capacity ratio. This can be referred to the depth of the first geogrid layer which has caused the whole reinforcing zone to be out of the range of the failure wedge. In fact, the failure wedge has been formed above the reinforcing zone in this condition (Figure 14). Whereas, in Figures 10 and 12, which shows the same results, an important role for both factors (n and h/B) is observed because of the smaller depth of the first geogrid layer.

4.4. Effect of the reinforcing depth

To study this factor, the variations of BCR$_u$ against d/B and h/B at $u/B = 0.25$ have been calculated and illustrated in Figure 15. It can be seen that in

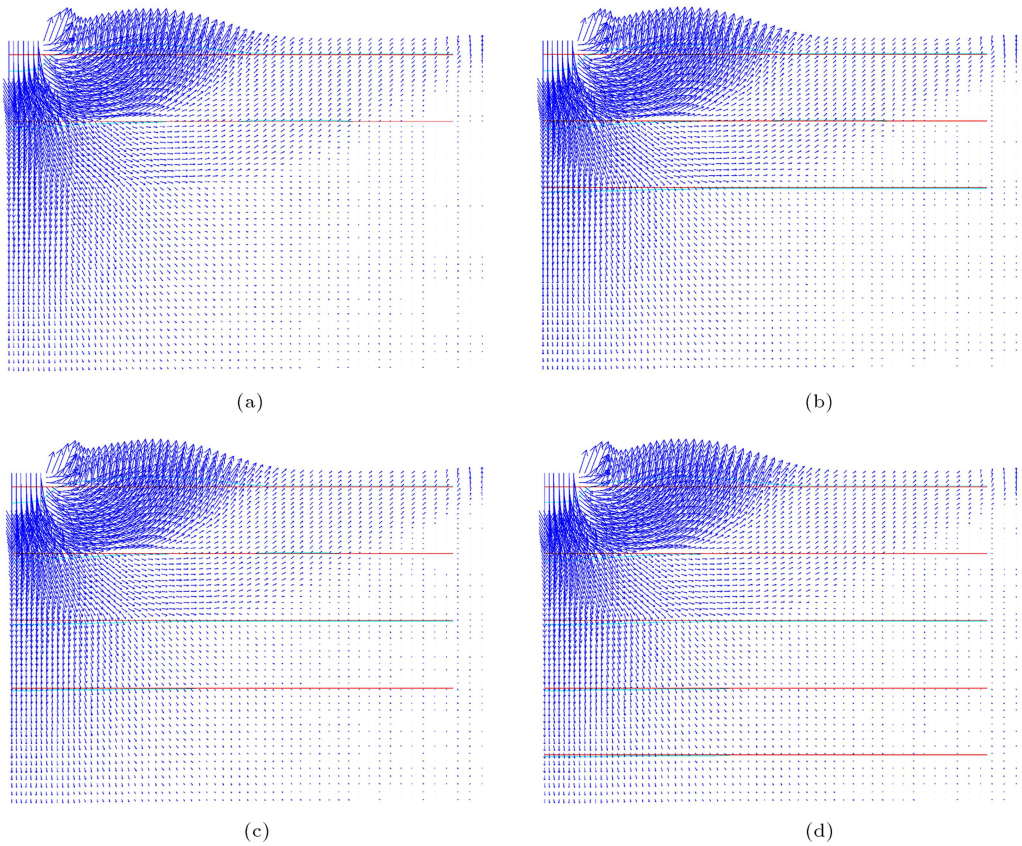

Figure 11. Displacement vectors of soil particles beneath the foundation, together with geogrid layers at $u/B = 0.25$ and $h/B = 1.25$: a) $n = 2$; b) $n = 3$; c) $n = 4$; and d) $n = 5$.

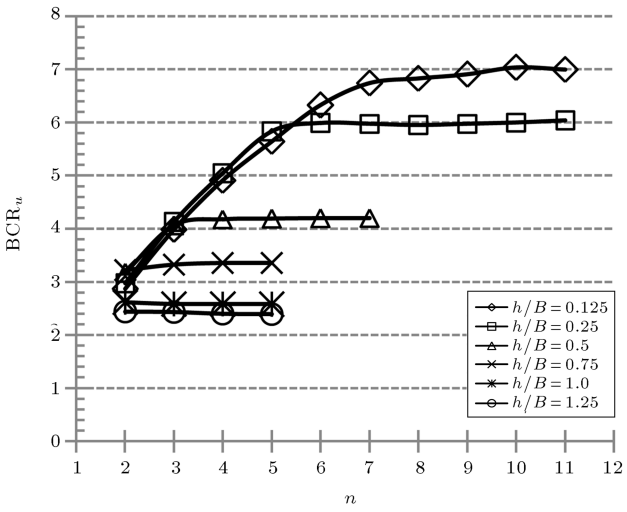

Figure 12. Variations of the ultimate bearing capacity ratio (BCR_u) versus number of the geogrid layers (n) for different spacing ratios (h/B) at $u/B = 0.5$.

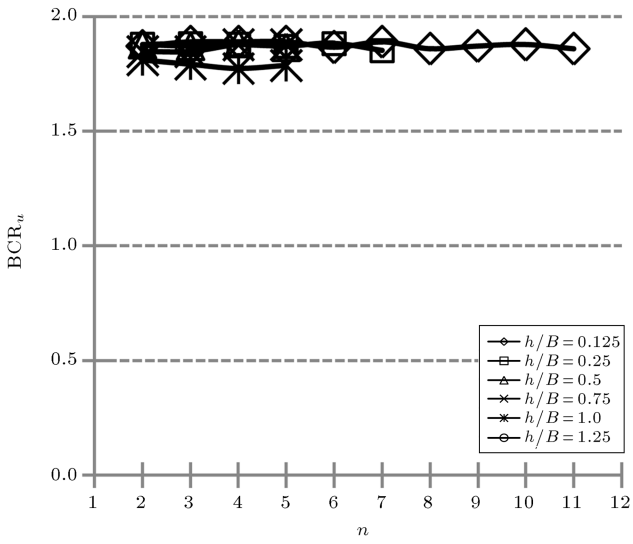

Figure 13. Variation of the ultimate bearing capacity ratio (BCR_u) versus number of the geogrid layers (n) for different spacing ratios (h/B) at $u/B = 1$.

many cases, the reinforcing depth of more than $1.75B$ has no effect on the bearing capacity improvement. Thus, in selecting the reinforcing depth, this should be taken into account. It can be observed that in case of $h/B = 0.125$, even for 11 layers of geogrid, the effective reinforcing depth is less than $1.75B$ still, and increasing the number of geogrid layers has considerable effect on the bearing capacity. As Figure 16 shows, the reason could be due to forming a stiff zone of reinforced soil beneath the foundation at an appropriate depth ($u/B = 0.25$).

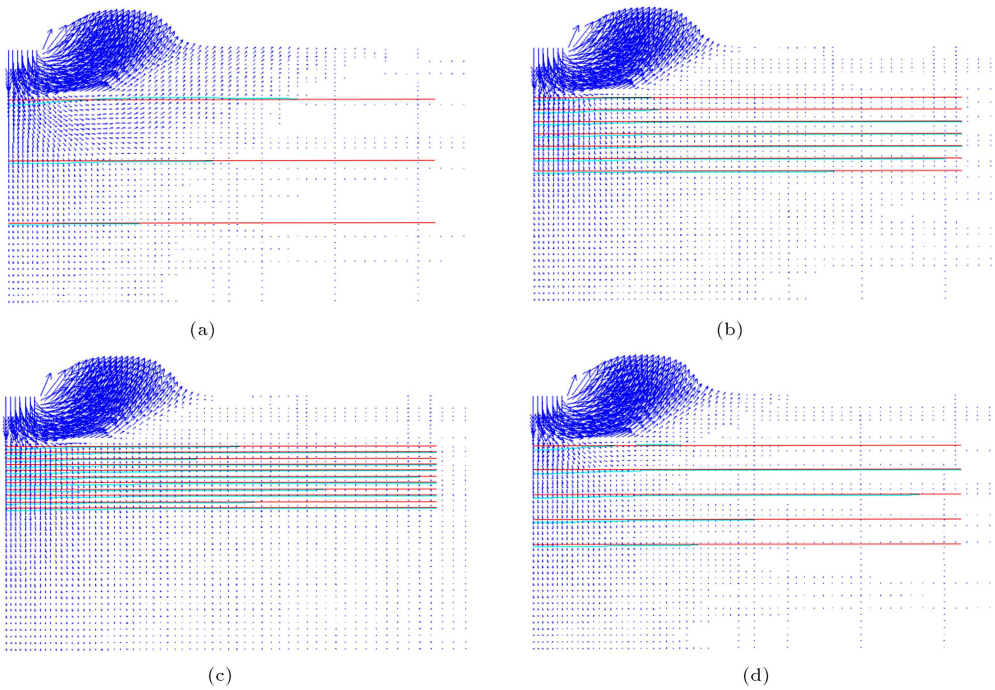

Figure 14. Displacement vectors of soil particles beneath foundation, together with the geogrid layers at $u/B = 1$: a) $n = 3$ and $h/B = 1.25$; b) $n = 7$ and $h/B = 0.25$; c) $n = 11$ and $h/B = 0.125$; and d) $n = 5$ and $h/B = 0.5$.

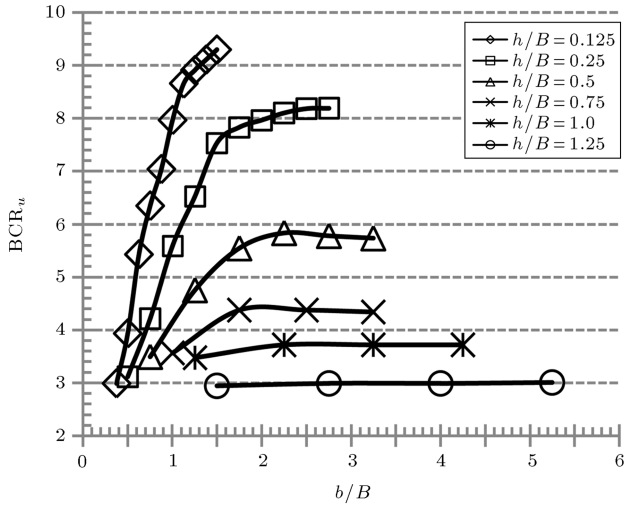

Figure 15. Variations of the ultimate bearing capacity ratio (BCR_u) versus reinforcing depth (d/B) for different spacing ratios (h/B) at $u/B = 0.25$.

For geogrid spacing of more than $0.25B$, the stiff zone is not formed, since the failure wedge will be formed incompletely between the geogrid layers. Figure 17 shows this fact for the geogrid spacing equal to $0.5B$. The results of the carried out analyses for $u/B = 0.25$ specify the optimum conditions in case of using a number of geogrid layers with spacing less than $0.5B$ ($h/B < 0.5$), as well as an appropriate reinforcing depth.

Variations of BCR_u versus d/B and h/B for $u/B = 0.5$ also show that for any geogrid distance, reinforcing depth more than $1.5B$ does not have any significant effect on the bearing capacity improvement (Figure 18). It can be concluded that for $u/B = 0.5$, in case of using multi-layers geogrid, taking the geogrid spacing less than half of the foundation width and reinforcing the soil in an appropriate depth lead to an optimum condition, and cause maximum improvement in the soil bearing capacity.

5. Summary and conclusion

The main factors, influencing the bearing capacity improvement, were investigated and presented in the case of geogrid reinforced soil. A strip footing on reinforced soil was numerically modeled using the FLAC-2D finite difference software. Extensive parametric analyses were implemented to study the soil-geogrid interaction, and to get the optimum condition for attaining the maximum bearing capacity improvements. Several qualitative and quantitative results were obtained as follows:

- The optimum depth of the first geogrid layer, regardless of the lower layers position, is $0.25B$, where B is the foundation width. For the depth more than $1.5B$, reinforcement will have no significant effect on the bearing capacity of the soil.
- The geogrid width and its tensile strength would have considerable effects on the bearing capacity improvement, if the depth of the first geogrid layer is less than $1B$.

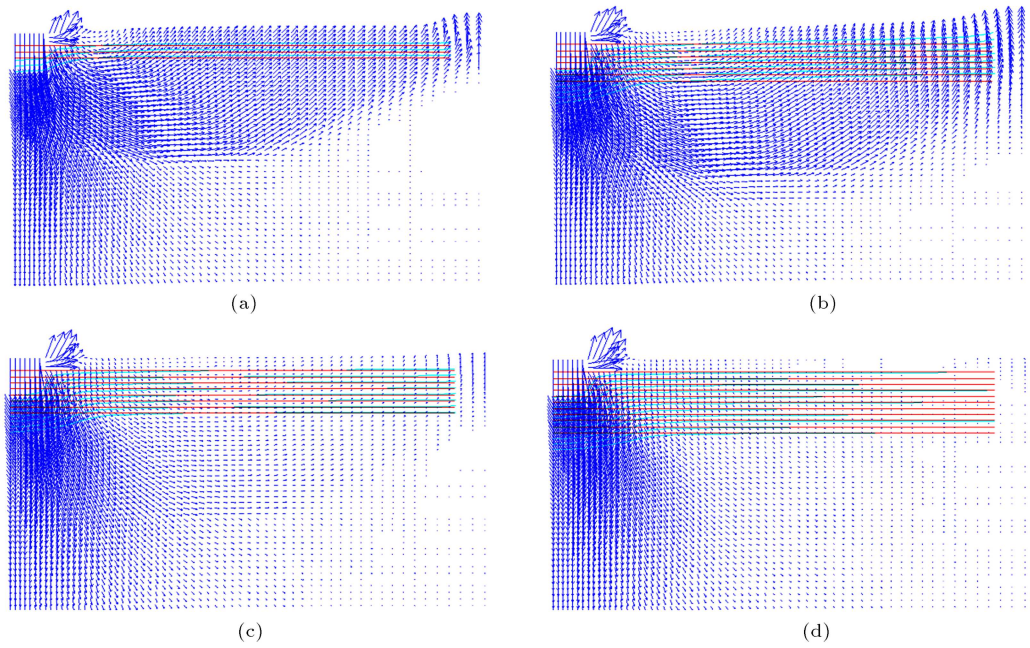

Figure 16. Displacement vectors of the soil particles beneath foundation together with the geogrid layers at $u/B = 0.25$ and $h/B = 0.125$: a) $n = 3$; b) $n = 7$; c) $n = 8$; and d) $n = 11$.

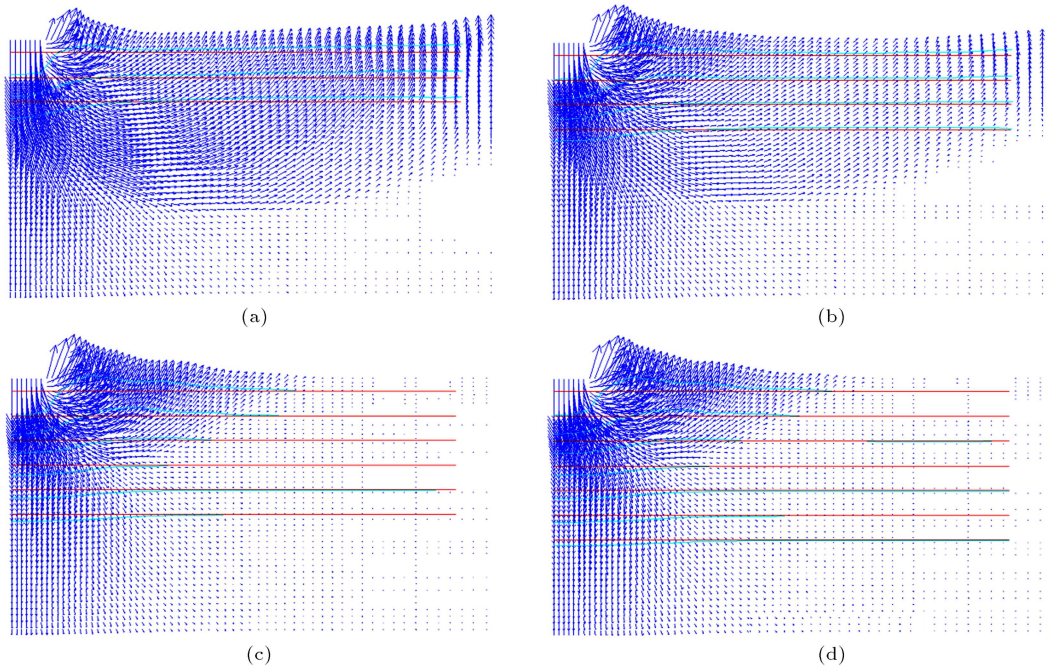

Figure 17. Displacement vectors of the soil particles beneath foundation together with the geogrid layers at $u/B = 0.25$ and $h/B = 0.5$: a) $n = 3$; b) $n = 4$; c) $n = 6$; and d) $n = 7$.

- The efficiency of reinforcement decreases significantly, if the geogrid width at an optimum depth is less than $10B$.
- Increasing the number of geogrid layers more than 2, when the spacing is greater than $1B$, would not have any effect on the soil bearing capacity.
- The optimum reinforcing depth is about $1.75B$. Increasing the number of geogrid layers in this depth by less than $0.5B$ spacing results in maximum efficiency of the reinforcement.
- Increasing the number of geogrid layers, while the depth of the first layer is more than $1B$, would have no effect on the bearing capacity improvement of the reinforced soil.

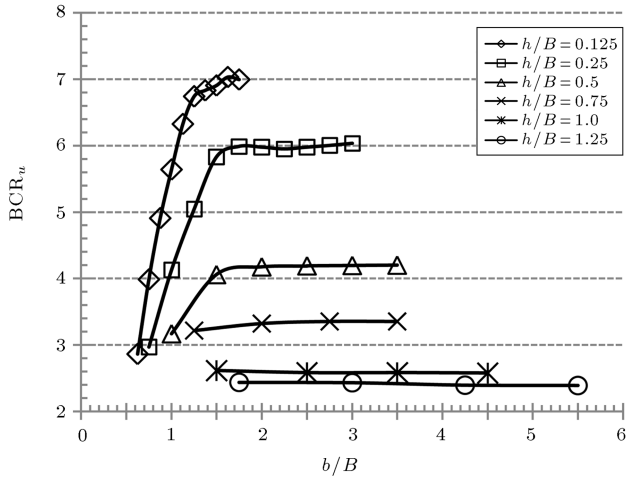

Figure 18. Variations of the ultimate bearing capacity ratio (BCR_u) versus the reinforcing depth ratio (d/B) for different spacing ratios (h/B) at $u/B = 0.5$.

References

1. Dash, S.K., Kroshnaswamy, N.R. and Rajagopal, K. "Bearing capacity of strip footings supported on geocell-reinforced sand", *Geotextiles and Geomembranes*, **19**, pp. 235-256 (2001).
2. Chung, W. and Cascante, G. "Experimental and numerical study of soil-reinforcement effects on the low-strain stiffness and bearing capacity of shallow foundations", *Geotechnical and Geological Engineering*, **25**, pp. 265-281 (2007).
3. Chen, Q. "An experimental study on characteristics and behavior of reinforced soil foundation", Ph.D. Dissertation, Louisiana State University, Baton Rouge, USA (2007).
4. Latha, G.M. and Somwanshi, A. "Effect of reinforcement form on the bearing capacity of square footings on sand", *Geotextiles and Geomembranes*, **27**, pp. 409-422 (2009).
5. Moghaddas Tafreshi, S.N. and Dawson, A.R. "Comparison of bearing capacity of a strip footing on sand with geocell and with planar forms of geotextile reinforcement", *Getextiles and Geomembranes*, **28**, pp. 72-84 (2010).
6. Lovisa, J., Shukla, S.K. and Sivakugan, N. "Behaviour of prestressed geotextile-reinforced sand bed supporting a loaded circular footing", *Geotextiles and Geomembranes*, **28**, pp. 23-32 (2010).
7. Binquet, J. and Lee, L.K. "Bearing capacity tests on reinforced earth mass", *J. Geotech. Eng. Div., ASCE*, **101**(12), pp. 1241-1255 (1975).
8. Huang, C.C. and Tatsuoka, F. "Bearing capacity of reinforced horizontal sandy ground", *Geotextiles & Geomembranes*, **9**, pp. 51-82 (1990).
9. Khing, K.H., Das, B.M., Puri, V.K., Cook, E.E. and Yen, S.C. "The bearing capacity of a strip foundation on geogrid-reinforced sand", *Geotextiles & Geomembranes*, **12**, pp. 351-361 (1993).
10. Omar, M.T., Das, B.M., Puri, V.K. and Yen, S.C. "Ultimate bearing capacity of shallow foundations on sand with geogrid reinforcement", *Canadian Geotech. J.*, **30**, pp. 545-549 (1993).
11. Shin, E.C. and Das, B.M. "Bearing capacity of strip foundation on geogrid-reinforced sand", *Proc. of the 11th Asian Regional Conf. on Soil Mech. and Geotech. Eng.*, pp. 189-192 (1999).
12. Shin, E.C., Das, B.M., Lee, E.S. and Atalar, C. "Bearing capacity of strip foundation on geogrid-reinforced sand", *Geotech. & Geological Eng.*, **20**, pp. 169-180 (2002).
13. Patra, C.R., Das, B.M. and Atalar, C. "Bearing capacity of embedded strip foundation on geogrid-reinforced sand", *Getextiles & Geomembranes*, **23**, pp. 454-462 (2005).
14. Kumar, A., Ohri, M.L. and Bansal, R.K. "Bearing capacity tests of strip footings on reinforced layered soil", *Geotech. and Geological Eng.*, **25**, pp. 139-150 (2007).
15. Basudhar, P.K., Dixit, P.M., Gharpure, A.D. and Deb, K. "Finite element analysis of geotextile-reinforced sand-bed subjected to strip loading", *Getextiles & Geomembranes*, **26**, pp. 91-99 (2008).
16. Sharma, R., Chen, Q., Abu-Farsakh, M. and Yoon, S. "Analytical modeling of geogrid reinforced soil foundation", *Geotextiles & Geomembranes*, **27**, pp. 63-72 (2009).
17. Abu-Farsakh, M., Chen, Q. and Sharma, R. "An experimental evaluation of the behavior of footings on geosynthetic-reinforced sand", *Soils and Foundations*, **53**, pp. 335-348 (2013).
18. Abrishami, S. "The study of cyclic bearing capacity of dry sands reinforced by geogrid using a physical model", Ph.D. Thesis, Amirkabir University of Technology, Tehran, Iran (2010).
19. Yin, J.H., Wang, Y.J. and Selvadurai, A.P.S. "Influence of nonassociativity on the bearing capacity of a strip footing", *Journal of Geotechnical and Geoenvironmental Eng. ASCE*, **127**(11), pp. 985-989 (2001).

Biographies

Seyed Majdedin Mir Mohammad Hosseini is a Professor of Geotechnical Engineering at Amirkabir University of Technology. He received his PhD in Geotechnical Earthquake Engineering from Leeds University in UK, and his MSc in Civil Engineering from Technical Faculty of Tehran University. His current and main research interests are: soil dynamics, geotech-

nical earthquake engineering, physical and numerical modeling in seismic soil behaviors and dynamic soil-structure interactions.

Mohammad Mahdi Salehi, MSc, was graduated in Geotechnical Engineering from Amirkabir University of Technology, Tehran, Iran. He received his BS degree from Isfahan University of Technology. His current research interests include soil improvement and numerical modeling of the soil structures.